Nonlinear coherent states of trapped-atom motion

Z. Kis,[1,*] W. Vogel,[1] and L. Davidovich[2]
[1]*Arbeitsgruppe Quantenoptik, Fachbereich Physik, Universität Rostock, Universitätsplatz 3, D-18051 Rostock, Germany*
[2]*Instituto de Física, Universidade Federal de Rio de Janeiro, Caixa Postal 68528, 21945-970 Rio de Janeiro, Rio de Janeiro, Brazil*
(Received 13 October 2000; published 1 August 2001)

The general character of nonlinear coherent states (NCS) is considered. A method is introduced by which any pure state of the quantum harmonic oscillator can be represented in a limiting sense as a NCS. The representation of a Fock state as a NCS is discussed in detail. As a physical example we show how to prepare a highly excited Fock state in an ion trap based on the concept of NCS.

DOI: 10.1103/PhysRevA.64.033401 PACS number(s): 42.50.Vk, 32.80.Qk, 42.50.Lc

I. INTRODUCTION

Nonclassical states of the electromagnetic field and of the atomic center-of-mass motion have played an important role in recent years, due to their relation with fundamental problems in quantum mechanics and to the many possible applications, ranging from high-resolution spectroscopy to low-noise communication and quantum computation. However, the generation of these states is usually a demanding experimental challenge. One of the most difficult tasks is the suppression of decoherence effects originating from the interaction of the quantum system under consideration with its environment. A particularly important system, where such decoherence effects can be suppressed to a level that allows one to prepare interesting quantum states, is composed of one or several trapped ions. In an ion trap the center-of-mass of a single ion experiences an approximate harmonic external potential [1], hence the ion trap is a realization of the harmonic oscillator model in quantum mechanics. Ion trapping inspired the development of laser cooling techniques such as ''Doppler'' laser cooling [2–4] and laser cooling in the resolved sideband limit [4], which allows one to prepare the ion in the vibrational ground state [5,6].

Making use of the momentum exchange between the atom and a driving light field, one can manipulate the atomic center-of-mass motion. In this manner, experiments have been performed that realize examples of squeezed states, motional number states [7], and Schrödinger-cat-like states [8]. These state-preparation methods typically rest on coherent interactions of the trapped atom with lasers that are appropriately tuned on particular vibronic transitions. Clearly such methods are limited by the decoherence mechanisms acting on the system. Since the decoherence effects become more important with increasing interaction time, the preparation of highly excited nonclassical states is expected to be difficult. For example, motional Fock states $|n\rangle$ have been experimentally prepared by sequences of n interactions with π pulses [7]. Thus the minimum required preparation time consists of $n/2$ Rabi cycles. On the other hand, in the experiments a significant damping of Rabi oscillations was observed on a time scale of several Rabi cycles. This decoherence is expected to substantially reduce the fidelity of Fock states prepared by this coherent scheme in cases where the quantum numbers are significantly larger than $n=10$.

To avoid the degradation of highly excited nonclassical states, one needs clear insight into the underlying decoherence mechanisms. In the case of the above experiments, the dominant source of decoherence of the Rabi oscillations, for an atom initially prepared in the motional ground state, has been shown to consist of rarely occurring spontaneous emissions from an auxiliary (far off resonant) electronic state that is used to enhance the Raman coupling strength of the lasers providing the coherent Rabi flopping [9]. Among the numerous experimental proposals for the generation of nonclassical motional states of a trapped ion, a remarkable class involves the generation of motional dark states. In this context the spontaneous emission, which usually limits the possibilities of coherent quantum-state preparation, serves a useful purpose: it is actually needed for preparing and stabilizing the nonclassical state under study. There are several theoretical proposals dealing with motional dark states that realize this type of dynamics, including squeezed states [10], even and odd coherent states [11], nonlinear coherent states (NCS) [12], and squeezed cat states [13]. Similarly, the generation of multimode entangled states as dark states could be also of practical importance. In this spirit, the preparation of pair coherent states [14], pair cat states [15], and approximate SU(2) states [16] have already been considered.

Out of the variety of dark states that can be realized, in the following we will be particularly interested in the NCS. It turns out that several notable states in quantum optics can be represented as NCS. For their properties see, e.g., Refs. [17,18]. Some special cases that have been considered are the q-deformed coherent states [19,20], the photon added coherent states [21] and the negative binomial states [22]. Several properties of the even and odd NCS have been discussed in Ref. [23], see also Ref. [24]. Other types of NCS have been considered in Refs. [25–27]. Whereas the preparation of some of the motional dark states is limited to the Lamb-Dicke regime, the NCS are insensitive even to the motional kick effects that become more and more important for large Lamb-Dicke parameters [12]. Thus their preparation in the form of dark states opens new possibilities for preparing highly excited nonclassical states that are almost undisturbed by spontaneous emission.

In the present paper we deal with the question of how

*Permanent address: Research Institute for Solid State Physics and Optics, H-1525 Budapest, P.O. Box 49, Hungary.

general the NCS are. We introduce explicitly a method by which, in a limiting sense, any pure state of the harmonic oscillator can be represented as a NCS. As an extreme example, we show that even the Fock states—although they do not display any coherence properties—belong to the class of NCS. Finally, we demonstrate by numerical simulations of the dark-state preparation method that the generation of highly excited motional Fock states of a single trapped ion, such as the state $|n=60\rangle$, is possible by making use of the concept of NCS.

This paper is organized as follows. In Sec. II the main properties of deformed harmonic oscillators are discussed. The definition of the deformed commutator relation and the coherent states associated with the deformed boson operators are summarized briefly in Sec. II A. In Sec. II B an important physical realization of the deformed boson operators is recalled, where the physical system is a single trapped ion driven by two laser fields and the spontaneous decay of the electronic state is included. It is shown in Sec. III that pure states of the harmonic oscillators can always be represented as NCS. In Sec. IV two representations of a Fock state as NCS are compared. The generation of a highly excited Fock state in an ion trap based on the concept of NCS is studied in Sec. V. A summary and some conclusions are given in Sec. VI.

II. DEFORMED HARMONIC OSCILLATOR

A. Deformed commutation relation

Deformations of the canonical commutation relations have been proposed since the early days of quantum mechanics [28]. For the harmonic oscillator, the usual creation and annihilation operators $\hat{a}^\dagger$ and $\hat{a}$ are replaced by deformed boson operators $\hat{A}^\dagger$ and $\hat{A}$, respectively [29–31]. A number operator $\hat{n}$ is also postulated which counts the quanta: $\hat{n}|n\rangle = n|n\rangle$. The set $\{|n\rangle; n=0,1,\ldots\}$ provides a denumerable basis for the Hilbert space (Fock space). The number operator satisfies

$$[\hat{n},\hat{A}]=-\hat{A} \quad \text{and} \quad [\hat{n},\hat{A}^\dagger]=\hat{A}^\dagger, \tag{1}$$

as for the usual nondeformed boson operators. Note that in this definition one does not require $\hat{A}$ and $\hat{A}^\dagger$ to be related to $\hat{n}$ in the usual way, i.e., in general $\hat{A}^\dagger\hat{A}\neq\hat{n}$. The vacuum state $|0\rangle$ does not contain quanta, therefore $\hat{n}|0\rangle=0$ and $\hat{A}|0\rangle = 0$. The product $\hat{A}^\dagger\hat{A}$ preserves the number of quanta, consequently it is necessarily a function of $\hat{n}$. A convenient notation of a *box* function is introduced $\hat{A}^\dagger\hat{A}=[\hat{n}]$ (read "box $\hat{n}$") [17]. Similarly, $\hat{A}\hat{A}^\dagger$ is also a function of $\hat{n}$ and it can be shown that $\hat{A}\hat{A}^\dagger=[\hat{n}+1]$. The deformed commutation relation is defined by

$$\hat{A}\hat{A}^\dagger-\hat{A}^\dagger\hat{A}=[\hat{n}+1]-[\hat{n}]. \tag{2}$$

One of the most important class of the deformed harmonic oscillator is the q-deformed oscillator. In case of "Maths" bosons

$$\hat{A}\hat{A}^\dagger-q\hat{A}^\dagger\hat{A}=1, \tag{3}$$

where q is some real number. This deformation was introduced in Ref. [29], where the corresponding q-coherent states, the eigenstates of the q-deformed annihilation operator $\hat{A}$, were also discussed. An equivalent commutator form (2) of the definition (3) can be derived [17], for which the *box* function reads

$$[n]=\frac{1-q^n}{1-q}. \tag{4}$$

The other most commonly used deformation of the commutation relation yields the "physics" bosons

$$\hat{A}\hat{A}^\dagger-q\hat{A}^\dagger\hat{A}=q^{-\hat{n}}. \tag{5}$$

This (P-case) deformation of the boson operators [19] is a realization of the Hopf algebras, or quantum groups [31]. For the commutator form (2) of the definition (5) the *box* function is given by [17]

$$[n]=\frac{\sinh(\lambda n)}{\sinh\lambda}, \quad \lambda=\ln q. \tag{6}$$

The q-deformed oscillators may be considered as special cases of the so-called f oscillators [18], where the f-oscillator operators have been defined by

$$\hat{A}=\hat{a}f(\hat{n}),$$

$$\hat{A}^\dagger=f(\hat{n})\hat{a}^\dagger. \tag{7}$$

The function $f(n)$ can be practically any real or complex-valued function. The basic commutator reads

$$[\hat{A},\hat{A}^\dagger]=(\hat{n}+1)f^2(\hat{n}+1)-\hat{n}f^2(\hat{n}). \tag{8}$$

It follows that $[n]=nf^2(n)$. By the special choice of the function $f(n)$

$$f(n)=\left(\frac{\sinh(\lambda n)}{n\sinh\lambda}\right)^{1/2}, \quad \lambda=\ln q \tag{9}$$

it has been shown that the q-deformed harmonic oscillator in the P case [cf. Eq. (5)] is a special case of the algebra of the f-oscillator operators Eq. (7). An important physical realization of the f oscillators is the center-of-mass motion of a trapped ion where the electronic system of the ion is subject to both radiative damping and resonant laser excitation at vibrational sidebands [12].

The coherent states associated with the deformed annihilation operator $\hat{A}$, are defined as

$$\hat{A}|\mu\rangle=\mu|\mu\rangle, \tag{10}$$

where μ is some complex number. These generalized coherent states are well defined if $|[n]/\mu^2|>1$ when $n\to\infty$. A re-

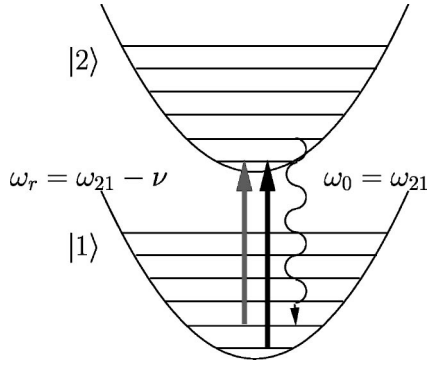

FIG. 1. Excitation scheme of the trapped ion for the preparation of a NCS.

lated expression in quantum optics has been considered in Refs. [17,32]. The expansion of the state $|\mu\rangle$ in the Fock basis is

$$|\mu\rangle = \mathcal{N}_\mu \sum_{n=0}^{\infty} \frac{\mu^n}{\sqrt{[n]!}} |n\rangle, \tag{11}$$

$$[n]! = [0][1]\cdots[n].$$

This solution of the eigenvalue equation (10) is very general, it can be adopted for all deformed boson operators which satisfy the deformed commutation relations (1),(2). The states of the form (11) are a generalization of the Fock representation of the coherent state. For the *f*-oscillators these states were also interpreted as NCS [12,18]. In the next subsection we discuss in more detail an ion trap system in which NCS emerge.

B. Nonlinear coherent states

The realization of a special class of NCS, corresponding to a special choice of the function $\hat{f}(\hat{n})$, has been proposed in the quantized motion of a trapped atom in a Paul trap [12]. We show in Fig. 1 the excitation scheme which will also be the basis for the generation of other types of NCS considered in the following. Two lasers drive the atom simultaneously in the resolved sideband regime. The first one of frequency ω_0 is resonant to the electronic carrier frequency ω_{21}. The second one of frequency ω_r is on resonance with the first red motional sideband, $\omega_r = \omega_{21} - \nu$, where ν is the motional frequency of the atom in the trap potential. Eventually, the wavy line in the scheme indicates a radiative decay of the excited electronic state with a decay rate Γ.

The dynamics of the system can be described by the master equation

$$\frac{d\hat{\varrho}}{dt} = -\frac{i}{\hbar}[\hat{H}_{\rm int}, \hat{\varrho}] + \frac{\Gamma}{2}(2\hat{A}_{12}\hat{\tilde{\varrho}}\hat{A}_{21} - \hat{A}_{22}\hat{\varrho} - \hat{\varrho}\hat{A}_{22}). \tag{12}$$

The operators $\hat{A}_{ji}$ flip the electronic state from $|i\rangle$ to $|j\rangle$ $(i,j=1,2)$. Moreover,

$$\hat{\tilde{\varrho}} = \frac{1}{2}\int_{-1}^{1} ds\, W(s) e^{i\eta s(\hat{a}+\hat{a}^\dagger)} \hat{\varrho} e^{-i\eta s(\hat{a}+\hat{a}^\dagger)} \tag{13}$$

includes the motional kick effects due to the emission of photons. The function $W(s)$ is the radiation pattern and the Lamb-Dicke parameter η measures the localization of the motional ground state of the atom relative to the (effective) wavelength of the transition. The Hamiltonian $\hat{H}_{\rm int}$ includes the two driving laser fields, each of which is described by a nonlinear Jaynes-Cummings Hamiltonian [33]

$$\hat{H}_{\rm int} = \frac{\hbar}{2}\{\Omega_r \eta_r f_1(\hat{n};\eta_r)\hat{a} + \Omega_0 f_0(\hat{n};\eta_0)\}\hat{A}_{21} + \text{H.c.}, \tag{14}$$

where Ω_q $(q=0,r)$ are the Rabi frequencies corresponding to the two laser fields, and

$$f_i(\hat{n};\eta) = e^{-\eta^2/2} \sum_{n=0}^{\infty} \frac{n!}{(n+i)!} L_n^{(i)}(\eta^2) |n\rangle\langle n|, \tag{15}$$

$L_n^{(i)}(x)$ being the associated Laguerre polynomial. Here the two Lamb-Dicke parameters are equal to each other $\eta_r = \eta_0$, since the laser fields propagate in parallel directions.

The steady state of the laser driven and damped atom is of the form

$$\hat{\varrho}_{\rm s} = |1\rangle|\psi\rangle\langle\psi|\langle 1|. \tag{16}$$

Since the atom is in the ground state, the motional state $|\psi\rangle$ is obtained when the atom stops to fluoresce, thus the system is said to be in a motional dark state [12]. Different types of motional dark states have been studied, such as squeezed states [10], even/odd coherent states [11], pair coherent states [14] and others. Driving the system according to the excitation scheme in Fig. 1 with two lasers of equal Lamb-Dicke parameters, the motional dark state shows up as a NCS [12],

$$|\psi\rangle \equiv |\chi; f\rangle, \tag{17}$$

which satisfies the eigenvalue equation

$$\hat{A}|\chi; f\rangle = \chi|\chi; f\rangle. \tag{18}$$

The deformed annihilation operator $\hat{A}$ is defined by

$$\hat{A} = f(\hat{n})\hat{a}. \tag{19}$$

Note that this definition is equivalent to that of the *f*-oscillator operators (7) since $f(\hat{n})\hat{a} = \hat{a}f(\hat{n}-1)$. In the following we will use the notation of $\hat{A}$ according to Eq. (19), which has the technical advantage of being in normally ordered form. In the ion trap system under consideration one obtains

$$\chi = \frac{i\Omega_0}{\eta\Omega_r}, \quad f(n) = \frac{L_n^{(1)}(\eta^2)}{(n+1)L_n^{(0)}(\eta^2)}. \tag{20}$$

Thus the eigenvalue χ can be well controlled by the two (complex) Rabi frequencies Ω_0 and Ω_r of the two lasers. The function $f(n)$ contains associated Laguerre polynomials and it can be partly modified via its dependence on η. These states may display interesting properties, such as amplitude squeezing and splitting into substates. In the latter case pronounced quantum interference effects can occur.

It would be of great interest if one could have more freedom to choose the form of the function $f(n)$ since in this case the NCS would include a wide class of pure quantum states. A possible way to tailor the function $f(n)$ in the ion trap is the engineering of the atom-laser interaction [34]. It allows one to control the excitation dependent nonlinearities by increasing the number of lasers driving the system. When the wave vectors of the lasers have different projections onto the motional degree of freedom of interest, the interaction is described by several Lamb-Dicke parameters that eventually allow one to control to some extent the function $f(n)$.

III. NCS REPRESENTATION OF PURE STATES

In this section we study the conditions for a state to belong to the class of NCS. The solution of the eigenvalue equation for the NCS [see Eq. (18)] can be expanded in terms of Fock states

$$\langle n|\chi;f\rangle=\mathcal{N}\frac{\chi^n}{\sqrt{n!}f(n-1)!}, \tag{21}$$

where we define

$$f(-1)!\equiv 1. \tag{22}$$

In order to express a state $|\psi\rangle$ as a NCS one may compare the Fock state expansion of the NCS in Eq. (21) with that of the state

$$|\psi\rangle=\sum_{n=0}^{\infty} c_n|n\rangle. \tag{23}$$

After some basic algebra one finds a relation between the Fock state coefficients of the state in question and the nonlinear function $f(n)$ of the NCS,

$$f(n)=\frac{\chi}{\sqrt{n+1}}\frac{c_n}{c_{n+1}}. \tag{24}$$

Inserting this function into Eqs. (18) together with Eq. (19), the resulting NCS is equal to the state $|\psi\rangle$ in Eq. (23), provided that $f(n)$ is a well-defined function.

Now we discuss the existence of the NCS determined by the function $f(n)$ in Eq. (24). If all coefficients c_n are nonzero in the Fock state expansion of the state $|\psi\rangle$ in Eq. (23) then $f(n)$ is a well-defined function for all $n\geqslant 0$. Certainly, in the limit of $n\to\infty$ it should be allowed that $|c_n|\to 0$, provided that the ratios $|c_n/c_{n+1}|$ remain finite. In other words, all the pure states $|\psi\rangle$ whose Fock state coefficients c_n are nonzero for any finite value of n belong to the class of NCS.

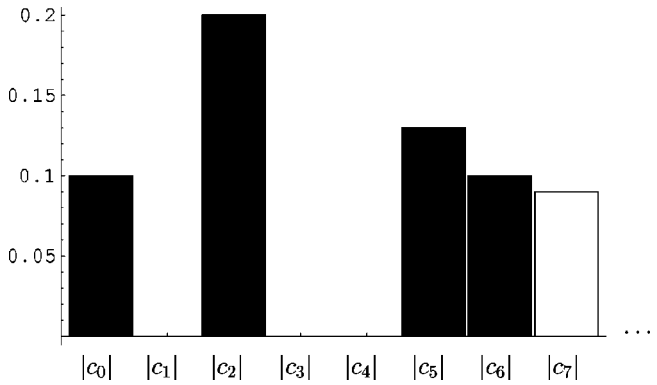

FIG. 2. The modulus of the first few Fock state expansion coefficients c_n of a state $|\psi\rangle$.

However, we encounter a problem if there are zeros in the expansion (23). To be more specific, let us consider the even Schrödinger-cat state

$$|\psi\rangle=\frac{1}{\mathcal{A}}(|\alpha\rangle+|-\alpha\rangle), \quad \mathcal{A}=\sqrt{2+2\exp(-2|\alpha|^2)}. \tag{25}$$

The Fock state coefficients of this state reads

$$c_n=\begin{cases}\dfrac{2}{\mathcal{A}}e^{-|\alpha|^2/2}\dfrac{\alpha^n}{\sqrt{n!}}, & n \text{ is even},\\ 0, & n \text{ is odd}.\end{cases} \tag{26}$$

As a result, we have a sequence of nonzero and zero coefficients. Inserting two consecutive c_n from Eq. (26) into Eq. (24) we get either zero or infinity for $f(n)$. Consequently, the function $f(n)$ is ill defined and the even Schrödinger-cat state does not belong in a strict sense to the class of NCS. More generally, if in the Fock state expansion of a state there are alternating zero and nonzero periods then the state does not belong in a strict sense to the class of NCS.

However, even if the function $f(n)$ is ill defined, it is possible to construct a NCS, in the sense of a limit, which may represent any chosen pure state. For this purpose we will consider the typical difficulties that may emerge in the NCS representation of an arbitrary pure state. In Fig. 2 we show the modulus of the first few Fock state coefficients of a state $|\psi\rangle$. Difficulties arise when a nonzero Fock state coefficient is followed by a zero one and vice versa, or if there are two or more coefficients one after the other which are zeros. In order to overcome these problems we propose to truncate the Hilbert space at an arbitrarily large but finite Fock state $|N\rangle$. The next step is to replace the zeros in the Fock state expansion of the state in question by ε/N where $\varepsilon\ll 1$ and fixed. We are going to construct a function $f(n)$ describing a state $|\chi;f\rangle_N$

$$|\chi;f\rangle_N=\mathcal{N}\sum_{n=0}^{N}\frac{\chi^n}{\sqrt{n!}f(n-1)!}|n\rangle, \tag{27}$$

which approximates the state $|\psi\rangle_N$ under consideration in the truncated Hilbert space.

In the following we give an example of the rules regarding the choice of the function $f(n)$.

R1. $c_n \neq 0$ and $c_{n+1} \neq 0$: apply Eq. (24).

R2. $c_n \neq 0$ and $c_{n+1} = 0$: replace c_{n+1} by ε/N then

$$f(n) = \frac{\chi}{\sqrt{n+1}} \frac{c_n}{\varepsilon/N}. \tag{28}$$

R3. $c_n = 0$ and $c_{n+1} \neq 0$: replace c_n by ε/N then

$$f(n) = \frac{\chi}{\sqrt{n+1}} \frac{\varepsilon/N}{c_{n+1}}, \tag{29}$$

R4. $c_n = 0$ and $c_{n+1} = 0$: replace both c_n and c_{n+1} by ε/N then

$$f(n) = \frac{\chi}{\sqrt{n+1}}, \tag{30}$$

where c_n, $(n = 0 \ldots N)$ are the Fock state coefficients of the state $|\psi\rangle$ in question. Note that the rule $R2$ describes a singular $f(n)$ as $N \to \infty$. The state $|\chi; f\rangle_N$ does not satisfy the eigenvalue equation (18), instead we have

$$\hat{A}|\chi; f\rangle_N = \chi(1 - |N\rangle\langle N|)|\chi; f\rangle_N, \tag{31}$$

where the last term on the right-hand side results from the truncation of the Hilbert space. As $N \to \infty$ this term vanishes since $\lim_{N\to\infty}(1 - |N\rangle\langle N|) = 1$.

It can be readily verified that if the function $f(n)$ satisfies the rules $R1 - R4$, then

$$|\psi\rangle_N \approx |\chi; f\rangle_N. \tag{32}$$

Taking the scalar product of both sides of this equation with the Fock state $|n\rangle$, $(n = 0, \ldots, N)$, one finds exact agreement for $\langle n|\psi\rangle_N \neq 0$. If on the left-hand side $\langle n|\psi\rangle_N = 0$ then on the right-hand side one obtains $\langle n|\chi; f\rangle_N = \varepsilon/N$. For a sufficiently large N this number can be arbitrarily small. The norm of the state $|\chi; f\rangle_N$ is

$${}_N\langle f; \chi|\chi; f\rangle_N = {}_N\langle\psi|\psi\rangle_N + k\frac{\varepsilon^2}{N^2}, \tag{33}$$

where k is the number of zeros out of the Fock state coefficients c_n, $(n = 0, \ldots, N)$ of the state $|\psi\rangle_N$. Since $k < N$ the relation $k\varepsilon^2/N^2 < \varepsilon^2/N$ holds, therefore the norm of $|\chi; f\rangle_N$ approaches 1 as $N \to \infty$. Taking the limit $N \to \infty$ one has

$$|\psi\rangle \equiv \lim_{N\to\infty} |\psi\rangle_N = \lim_{N\to\infty} |\chi; f\rangle_N \equiv |\chi; f\rangle. \tag{34}$$

The last equation means that in the limit of $N \to \infty$ the state $|\chi; f\rangle_N$ will be the NCS $|\chi; f\rangle$, which satisfies the eigenvalue equation (18). In this way the method yields a NCS which is equivalent to the state under consideration.

We should note that the method discussed above is not the only one by which an arbitrary state $|\psi\rangle$ can be represented as a limit of a NCS. Our intention is to demonstrate that such a method can be constructed, and to consider the mathematical problems that arise in the course of the construction of such a method. In the next section we discuss a case of particular interest, the representation of a Fock state as a NCS. For the Fock state all but one coefficient c_n are vanishing. Moreover, they are known to display no coherence properties. In this sense the Fock states may be expected to be the most unlikely to belong to the class of NCS. It is interesting that, nevertheless, they can be represented in the form of NCS.

IV. REPRESENTING FOCK STATES AS NCS

In this section we will show that Fock states belong, as a limiting case, to the class of NCS. To represent a Fock state the function $f(m)$ should satisfy the condition [we denote this function in the following by $f_\varepsilon(m)$, in order to make explicit the dependence on the parameter ε]:

$$\frac{1}{f_\varepsilon(n-1)!} \approx \begin{cases} 1/\varepsilon, & n = k, \\ \ll 1/\varepsilon, & n \neq k, \end{cases} \tag{35}$$

where $\varepsilon \ll 1$ is a small number. In the NCS determined by this function $f_\varepsilon^{-1}(m)$ the coefficient of the kth Fock state exceeds by orders of magnitudes all the others, hence after renormalization one gets with very good approximation the Fock state $|k\rangle$. Indeed, taking the limit $\varepsilon \to 0$ one finds

$$\lim_{\varepsilon\to 0} |\chi; f_\varepsilon\rangle = |k\rangle, \tag{36}$$

where $|\chi; f_\varepsilon\rangle$ is defined in Eq. (21). Note, that in Eq. (36) the limiting state is the Fock state $|k\rangle$ for any finite, nonvanishing value of χ. The function $f_\varepsilon^{-1}(m)$ could be realized by choosing

$$f_\varepsilon^{-1}(m) = \frac{k - m - \varepsilon}{m - k + 1 + \varepsilon}. \tag{37}$$

This function takes finite values for $m < k - 1$, and for $\varepsilon \ll 1$ it has an effective cutoff for $m \geqslant k$.

So far we have dealt with the mathematical representation of a Fock state as a NCS. However, it has been shown in Ref. [35] that under ideal conditions a Fock state can be prepared as a dark motional state of a trapped ion. In the proposed scheme the atom is driven by two lasers in different directions, so that the Lamb-Dicke parameters on the carrier and the red sidebands η_0 and η_r, respectively, can be varied independently of each other. Expanding the steady state of the system in the Fock basis Eq. (23), from the master equation (12) together with the ansatz (16) one may derive the recursion relation [35]

$$\frac{e^{-\eta_r^2/2}}{\sqrt{m+1}} L_m^{(1)}(\eta_r^2) c_{m+1} + \chi e^{-\eta_0^2/2} L_m^{(0)}(\eta_0^2) c_m = 0. \tag{38}$$

One may choose the LD parameter η_0 such that $L_m^{(0)}(\eta_0^2)=0$ for $m=k$. In this case the recursion relation ensures that all coefficients c_m vanish for $m>k$. Moreover, one may fix η_r such that $L_{k-1}^{(1)}(\eta_r^2)=0$. As a consequence all c_m vanish for $m<k$. The conclusion is that the only nonvanishing coefficient is c_k and thus the steady state of the atomic motion is the kth Fock state

$$|\psi\rangle \equiv |k\rangle. \tag{39}$$

We emphasize that in order to get the Fock state $|k\rangle$ as the solution of the recursion relation (38), the LD parameters should be set with extremely high precision as we will see later.

We point out that the states defined by the recursion relation (38) are in fact nonlinear coherent states. In the general case of arbitrary values of the LD parameters the recursion relation (38) yields

$$|\psi\rangle \equiv |\chi; f\rangle,$$

$$f^{-1}(m) = \frac{(m+1)L_m^{(0)}(\eta_0^2)}{L_m^{(1)}(\eta_r^2)} e^{(\eta_r^2-\eta_0^2)/2}. \tag{40}$$

By choosing the LD parameters according to the discussion given above the NCS (40) is equivalent to the Fock state $|k\rangle$. Since it is impossible in an experiment to fix precisely the value of the LD parameters, it is of interest whether the realization of Fock states as NCS becomes possible under more realistic conditions.

So far we have discussed two representations of a Fock state as NCS: one of them is derived from pure mathematical considerations [see Eqs (35),(36)], the other one represents the motional state of an appropriately driven trapped ion [see Eq. (40)] under idealized conditions. We show now that these two representations are similar to each other, but not equivalent. Expanding the function for the trapped atom, Eq. (40), around the zeros chosen to get the kth Fock state, we arrive at

$$f^{-1}(m) \propto \frac{L_m^{(0)}(\eta_0^2)}{L_m^{(1)}(\eta_1^2)} \approx \frac{a(m-k)+L_k^{(0)}(\eta_0^2)}{b(m-k+1)+L_{k-1}^{(1)}(\eta_r^2)}, \tag{41}$$

where we allow the LD parameters η_0 and η_r not to take their precise values, i.e., the corresponding Laguerre polynomials are not exactly equal to zero at these points. It can be seen that the expansion of $f^{-1}(m)$ around $m=k$ in Eq. (41) is a rescaled version of $f_\varepsilon^{-1}(m)$ in Eq. (37). In Fig. 3 we compare these two functions, which exhibit a similar behavior. Most importantly, they are strongly peaked at $m=k$, which cannot be seen in the figure, since the height of the peaks could be even infinite in principle. Here we have chosen η_0^2 and η_r^2 such that they agree for 50 digits with the precise lowest roots of $L_k^{(0)}(x)$ and $L_{k-1}^{(1)}(x)$, respectively.

In Fig. 4 we redisplay $f^{-1}(m)$ and $f_\varepsilon^{-1}(m)$ for a larger m interval. The function $f_\varepsilon^{-1}(m)$ behaves as expected, it becomes constant far from its singularity. However, the function $f^{-1}(m)$ exhibits several peaks. These peaks emerge because $L_m^{(1)}(\eta_r^2)$ is almost zero not only for $m=k-1$, but for several larger values of m too. Under the chosen conditions the heights of the secondary peaks are of the order of few hundreds compared to the value of 10^6 of the main peak. A natural question arises: how sensitive are the results of the recursion relation (38), or equivalently the NCS (40), with respect to the chosen precision of the calculation, and thus with respect to the precision of an experiment. Using MATHEMATICA [36], we have evaluated Eq. (40) with the extreme precision of 50 digits. The LD parameters η_0 and η_r were chosen in such a way that their first 50 digits were equal to the square root of the roots of the Laguerre polynomials $L_k^{(0)}(x)$ and $L_{k-1}^{(1)}(x)$, respectively.

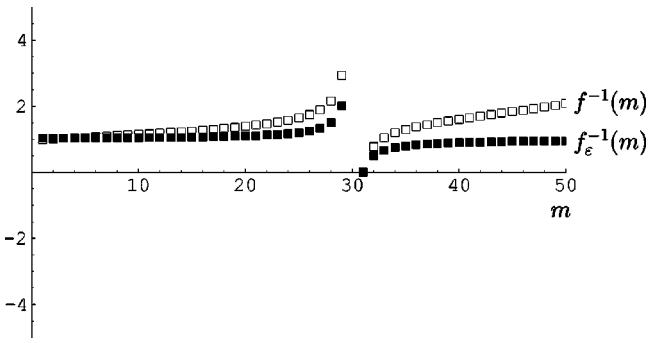

FIG. 3. The behavior of the functions $f_\varepsilon^{-1}(m)$ (filled boxes) and $f^{-1}(m)$ (empty boxes) defined in Eqs. (37) and (40), respectively, around their singularities. These functions correspond to the Fock state $|30\rangle$.

The result is shown in Fig. 5. It can be seen that the emerging state depends sensitively on the choice of the eigenvalue χ. In all cases we did not obtain the expected Fock state, but a state which is a superposition of several Fock states. This means that performing the calculations with even extremely large but finite precision prevents us to obtain the Fock states as predicted by the recursion relation (38). Consequently, getting a Fock state with Eq. (40) is a mathemati-

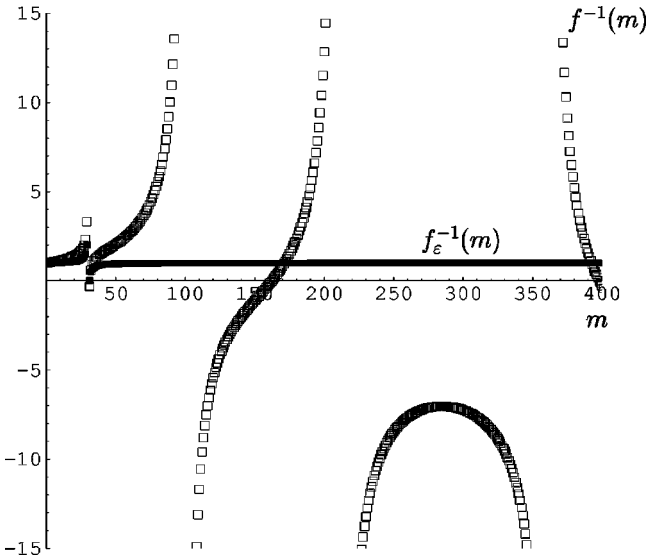

FIG. 4. Same as Fig. 3 but for a longer interval.

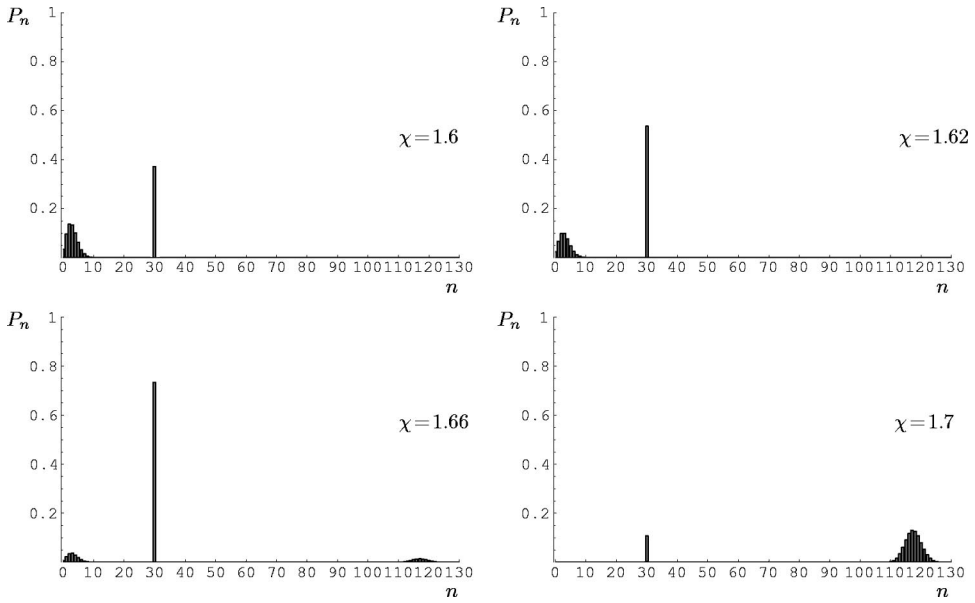

FIG. 5. The motional number statistics P_n is shown for the stationary states resulting from the recursion relation (38) for four different values of the eigenvalue χ. The calculations were performed with 50 digits of precision.

cally unstable procedure. This instability occurs in the determination of the steady state. In practice, however, the time needed to approach this steady state may be extremely large. Thus, it may be possible, despite the instability of the steady state, that in the laboratory one can actually prepare, through the NCS method, a highly excited Fock state as a quasistationary state. The physical reason for this possibility results from the fact that the different regions of the Hilbert space contributing to the steady state are coupled very weakly by both the driving lasers and the momentum transfer on the atom due to spontaneous emission. In fact, we will show that it is possible to generate a Fock state in a laser-driven trapped ion system by using the idea of independent adjustment of the LD parameters of the carrier and sideband lasers. In the next section we discuss an experimental scheme, in which the problems arising from the additional peaks of $f^{-1}(m)$ are avoided by effectively truncating the Hilbert space of the system in the dynamics.

In an experiment the LD parameters cannot be controlled with arbitrary precision. From recent experiments it appears to be reasonable that the LD parameters can be fixed with 3 digits of precision [37]. This loss of accuracy may result in a significant mismatch between the roots of the Laguerre polynomials and the squares of the LD parameters. The main effect of this deviation is the diminution of the height of the peak of the function $f^{-1}(m)$ at $m=k-1$, as one expects from Eq. (41). The other peaks remain unaltered practically. The reduction of the important peak of $f^{-1}(m)$ compared to the others will decrease further the quality of the ''Fock state'' which was supposed to be obtained from the recursion relation (38).

V. GENERATION OF A FOCK STATE BASED ON THE CONCEPT OF NCS

In the previous section we have compared two representations of a Fock state as NCS. One of them being derived from purely mathematical considerations, the other one originating from the motional state of a trapped ion which is driven by laser fields. We have demonstrated that the latter one is mathematically unstable due to the multipeak structure of the function $f^{-1}(n)$ in Eq. (40). In this section we are going to show that in spite of this instability, the ion may reach a highly excited Fock state in the NCS preparation scheme, by making use of the dynamics of the ion together with appropriately chosen initial vibrational states and LD parameters.

The master equation governing the time evolution of the density operator $\hat{\varrho}(t)$ of a trapped ion, which suffers spontaneous decay of level 2, and is subject to a bichromatic laser excitation of Jaynes-Cummings type, has already been discussed in Sec. II B and is redisplayed here for convenience:

$$\frac{d\hat{\varrho}}{dt}=-\frac{i}{\hbar}[\hat{H}_{\rm int},\hat{\varrho}]+\frac{\Gamma}{2}(2\hat{A}_{12}\hat{\tilde{\varrho}}\hat{A}_{21}-\hat{A}_{22}\hat{\varrho}-\hat{\varrho}\hat{A}_{22}). \tag{42}$$

The recoil term $\hat{\tilde{\varrho}}$ in the dissipative part is defined in Eq. (13). Similarly to the original idea for preparing NCS [12] two laser fields are applied. One of them is tuned to the carrier frequency of the electronic transition and the other one is tuned to the first red vibrational sideband. Now the LD parameters η_0 and η_r associated with the fields at the carrier frequency and at the first red vibrational sidebands, respectively, are chosen independently of each other by varying the direction of the laser fields. The Hamiltonian $\hat{H}_{\rm int}$ is given by Eq. (14). The stationary solution of the master equation (42) has the form given in Eq. (16), where the vibrational part $|\psi\rangle$ is given in Eq. (40).

In a numerical simulation the Fock space is necessarily truncated. If we look for the solution of the recursion relation (38) in a truncated Fock space of dimension N, provided that N is between the first and second approximate singularity of the function $f^{-1}(m)$ [see Eq. (40)], then the problem with the multipeak structure of $f^{-1}(m)$ is avoided. It can be verified numerically that the resulting state will be the assumed Fock state for a wide range of the eigenvalue χ. In the ex-

amples discussed below we will see that in the dynamics one in fact effectively has such a truncated Hilbert space if the initial state of the system is chosen appropriately.

The time evolution of the density operator was calculated by a quantum trajectory method [38–40]. The effective, non-Hermitian Hamiltonian governing the continuous dynamics reads

$$\hat{H}_{\rm eff}=\hat{H}_{\rm int}-i\frac{\hbar\Gamma}{2}\hat{A}_{22}, \tag{43}$$

where $\hat{H}_{\rm int}$ is defined in Eq. (14) and the jump operators are given by

$$\hat{J}_u=\sqrt{\Gamma w(u)}\hat{A}_{12}e^{iuk_{21}\hat{x}(t)}. \tag{44}$$

In the course of quantum trajectory simulations an initial wave function is evolved with the Hamiltonian $\hat{H}_{\rm eff}$ and jumps at random times interrupt this evolution. The times of the jumps are determined by the decay of the norm of the time-evolved wave function.

In the first numerical example the initial state was set as

$$|\Psi\rangle_{\rm in}=|1\rangle|0\rangle, \tag{45}$$

representing an ion in the ground electronic state $|1\rangle$ and vibrational state $|0\rangle$. The LD parameters $\eta_0=0.155$ and $\eta_r=0.247$ were chosen so that the vibrational part of the stationary solution (16) of the master equation (42) was (in the truncated Hilbert space) the Fock state $|60\rangle$. However, the precision of the LD parameters was only three digits. The dimension of the Fock space in the simulation was $N=70$. The eigenvalue $\chi=3.5$ was chosen so that the recursion relation (38) yields the required target state in the truncated Fock space. The order of magnitude of the interaction strengths $\Omega_0=2.6\Gamma$, $\Omega_r=3\Gamma$ in the Hamiltonian (14) was the same as the relaxation rate Γ. The duration of the time evolution was $\Gamma t=300$, on this time scale the evolution of the density operator $\hat{\varrho}(t)$ has practically stopped as it can be seen in Fig. 6. We have verified numerically that the density operator remains unchanged even on a longer time scale of $\Gamma t=2000$. The resulting vibrational distribution is shown in Fig. 7. This state is very far from the Fock state $|60\rangle$. If we compare with the behavior of the steady state in the case of the target state $|30\rangle$, Fig. 5, we have obtained additional peaks in the number statistics that were different from the target state. In the dynamics, where the system was initially in the motional ground state, the first peak appears to be populated. The coupling from this distribution to the wanted dark state is very weak, which is reflected by the nearly stationary behavior obtained in Fig. 6. Even if the target state would be reached on a much longer time scale this would be of limited practical relevance. In experiments technical noise effects play an increasing role for longer interaction times, which would prevent the system from approaching the target state.

In our second numerical simulation the initial state was a coherent motional state in the electronic ground state

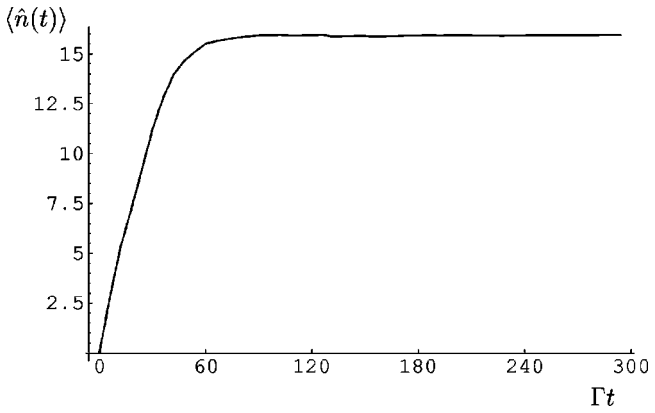

FIG. 6. The time evolution of the mean value of the vibrational population for the ion in the electronic ground state. Initially, the system was in the electronic and vibrational ground state and the target vibrational state was the Fock state $|60\rangle$, which is not reached on the considered time scale (the scaled time Γt is dimensionless).

$$|\Psi\rangle_{\rm in}=|1\rangle|\alpha\rangle \tag{46}$$

with $|\alpha|=7$. The dimension of the Fock space was $N=120$, all the other parameters were set as it was in the first example. The coherent state $|\alpha=7\rangle$ has a mean Fock-state occupation $\bar{n}=49$. In this case the main part of the initial distribution is below the target Fock state $|60\rangle$. We have performed a similar numerical simulation as in the previous case to obtain the time-evolved density operator $\hat{\varrho}(t)$. After a time interval of $\Gamma t=1500$ the resulting Fock-state distribution is shown in Fig. 8. This distribution consists of two parts: one of them is centered around the target Fock state $|60\rangle$, the other one is situated in the same region as in the previous example where the initial vibrational state was the vacuum $|0\rangle$. However, now the occupation of the target vibrational state is quite large $P_{60}=0.811$.

In the third numerical example we chose the initial state according to Eq. (46) with $|\alpha|=9$. All the other conditions are the same as in the previous case. The coherent state $|\alpha=9\rangle$ has a mean Fock-state occupation $\bar{n}=81$. It follows that

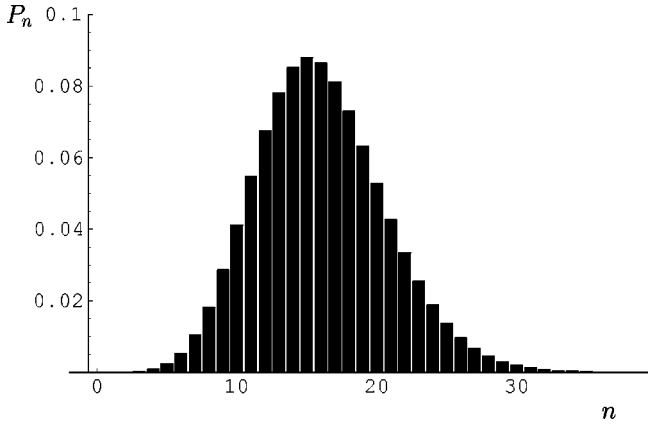

FIG. 7. The population distribution of the vibrational state for the ion in the electronic ground state after a time evolution of $\Gamma t=2000$. The physical conditions are the same as in Fig. 6.

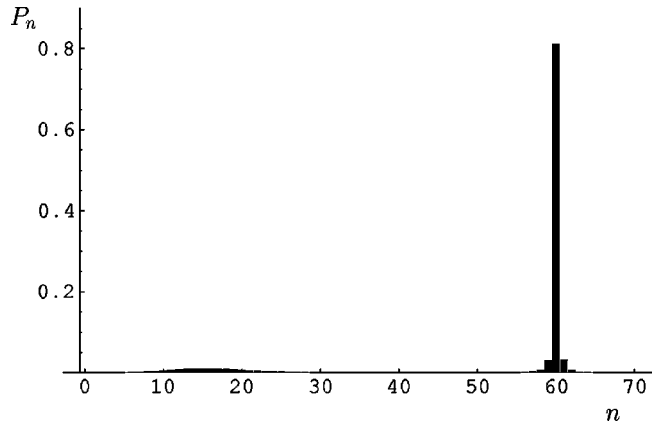

FIG. 8. Same as Fig. 7. The initial state was the coherent state $|\alpha\rangle$ with $|\alpha|=7$.

the main part of the initial distribution was above the target Fock state $|60\rangle$. The evolution of the Fock-state distribution derived from the density operator $\hat{\varrho}(t)$ [see Eq. (42)] is shown in Fig. 9 for several values of Γt. It can be clearly seen that the initial distribution moves towards the target Fock state while it gets narrower. Because of the weakness of the dynamical coupling with higher-order Fock states, the Hilbert space is effectively truncated to suppress contributions to the quasistationary states above the target Fock state $|60\rangle$. This dynamical truncation provides the necessary condition for the steady state solutions discussed in the previous section. The population of the target vibrational state is $P_{60}=0.95$ at $\Gamma t=1300$. This state is almost a perfect Fock state. Compared to the previous example, where the initial state was a coherent state with mean population number below the target Fock state, now we got a higher population for the target vibrational state on a shorter time scale.

The results of the previous three numerical examples can be summarized as follows: if the initial vibrational state has a narrow Fock-state distribution and is situated close to the target Fock state the system will reach the target state with high probability on a reasonable time scale. If the initial vibrational distribution is far below the target Fock state the system does not evolve to the desired target state in a reasonable time. In particular it turns out to be useful to choose the initial motional state somewhat above the target state. This is not surprising since the action of the laser on the red sideband in connection with spontaneous emission has a tendency to cool the motional subsystem. The numerical simulations also show that the dynamics effectively truncates the Hilbert space of the ion motion so that the time evolution of the system results in a quasistationary Fock state. The considered method of preparing highly excited motional Fock states in the form of NCS may be feasible for trapped ion experiments.

VI. SUMMARY AND CONCLUSIONS

We have studied under which circumstances a pure state of the harmonic oscillator belongs to the class of NCS. All those states having nonzero expansion coefficients in the Fock representation can always be expressed in the form of NCS. Moreover, it has been shown that even if there are zeros in the expansion of a given quantum state, it can be represented as a NCS in the sense of a limit. As an extreme example the representation of a Fock state as a NCS has been considered. We have provided a representation based on purely mathematical considerations and have discussed a representation originating from the motional dark states of a laser-driven trapped ion. We have shown that, while the first representation is mathematically stable, the latter turns out to be unstable. In this case a Fock state can be obtained only if the Hilbert space of the oscillator is appropriately truncated.

Nevertheless, we have shown that even highly excited Fock states can be generated in ion traps based on the concept of NCS. The reason for this possibility can be seen in

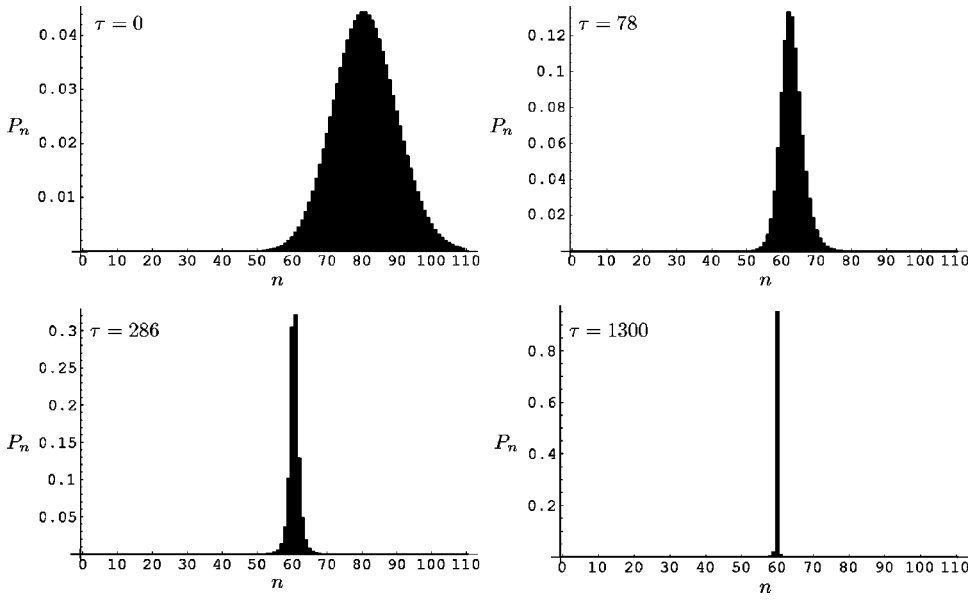

FIG. 9. The time evolution of the motional number statistics for an initial coherent state $|\alpha=9\rangle$. The scaled time is given by $\tau=\Gamma t$.

the extremely weak coupling between the distinct regions of the Hilbert space in which substantial contributions to the motional dark state are expected to occur. This results in an effective cutoff in the Hilbert space of the center-of-mass motion of the ion. The dynamical evolution of the system has been studied by quantum trajectory methods. It has been shown that, if the initial vibrational state has a narrow Fock-state distribution and it is situated close to the target Fock state, the system will reach the target state with high probability on a reasonable time scale.

ACKNOWLEDGMENTS

This work was supported by Deutscher Akademischer Austauschdienst (DAAD), Deutsche Forschungsgemeinschaft (DFG), Coordenação de Aperfeiçoamento de Pessoal de Ensino Superior (CAPES), Conselho Nacional de Desenvolvimento Científico e Tecnológico (CNPq), Fundação de Amparo à Pesquisa do Estado do Rio de Janeiro (FAPERJ), Fundação Universitária José Bonifácio (FUJB), and Programa de Apoio a Núcleos de Excelência (PRONEX).

[1] P.K. Ghosh, *Ion Traps* (Clarendon, Oxford, 1995).
[2] D.J. Wineland, R.E. Drullinger, and F.L. Walls, Phys. Rev. Lett. **40**, 1639 (1978).
[3] W. Neuhauser, M. Hohenstatt, P. Toschek, and H. Dehmelt, Phys. Rev. Lett. **41**, 233 (1978).
[4] D.J. Wineland and W.M. Itano, Phys. Rev. A **20**, 1521 (1979).
[5] F. Diedrich, J.C. Bergquist, W.M. Itano, and D.J. Wineland, Phys. Rev. Lett. **62**, 403 (1989).
[6] C. Monroe, D.M. Meekhof, B.E. King, S.R. Jefferts, W.M. Itano, D.J. Wineland, and P. Gould, Phys. Rev. Lett. **75**, 4011 (1995).
[7] D.M. Meekhof, C. Monroe, B.E. King, W.M. Itano, and D.J. Wineland, Phys. Rev. Lett. **76**, 1796 (1996).
[8] C. Monroe, D.M. Meekhof, B. E. King, and D. Wineland, Science **272**, 1131 (1996).
[9] C. Di Fidio and W. Vogel, Phys. Rev. A **62**, 031802(R) (2000).
[10] J.I. Cirac, A.S. Parkins, R. Blatt, and P. Zoller, Phys. Rev. Lett. **70**, 556 (1993).
[11] R.L. de Matos Filho and W. Vogel, Phys. Rev. Lett. **76**, 608 (1996).
[12] R.L. de Matos Filho and W. Vogel, Phys. Rev. A **54**, 4560 (1996).
[13] S.-C. Gou, J. Steinbach, and P.L. Knight, Phys. Rev. A **55**, 3719 (1997).
[14] S.-C. Gou, J. Steinbach, and P.L. Knight, Phys. Rev. A **54**, R1014 (1996).
[15] S.-C. Gou, J. Steinbach, and P.L. Knight, Phys. Rev. A **54**, 4315 (1996).
[16] Z. Kis, W. Vogel, L. Davidovich, and N. Zagury, Phys. Rev. A **63**, 053410 (2001).
[17] A.I. Solomon, Phys. Lett. A **196**, 29 (1994).
[18] V.I. Man'ko, G. Marmo, E.C.G. Sudarshan, and F. Zaccaria, Phys. Scr. **55**, 528 (1997); V.I. Man'ko and R. Vilela Mendes, J. Phys. A **31**, 6037 (1998).
[19] L.C. Biedenharn, J. Phys. A **22**, L873 (1989); A. Macfarlane, *ibid.* **22**, 4581 (1989).
[20] V.I. Man'ko, G. Marmo, S. Solimeno, and F. Zaccaria, Int. J. Mod. Phys. A **8**, 3577 (1993); V.I. Man'ko, G. Marmo, S. Solimeno, and F. Zaccaria, Phys. Lett. A **176**, 173 (1993).
[21] S. Sivakumar, J. Phys. A **32**, 3441 (1999).
[22] X.-G. Wang and H.-C. Fu, Mod. Phys. Lett. B **13**, 617 (1999).
[23] S. Mancini, Phys. Lett. A **233**, 291 (1997); B. Roy and P. Roy, *ibid.* **257**, 264 (1999).
[24] B. Roy, Phys. Lett. A **249**, 25 (1998).
[25] G. Junker and P. Roy, Phys. Lett. A **257**, 113 (1999).
[26] K.A. Penson and A.I. Solomon, J. Math. Phys. **40**, 2354 (1999).
[27] J.-M. Sixdeniers, K.A. Penson, and A.I. Solomon, J. Phys. A **32**, 7543 (1999).
[28] H.P. Dürr, *Werner Heisenberg und die Physik unserer Zeit* (Vieweg, Braunschweig, 1961); H. Rampacher, H. Stumpf, and F. Wagner, Fortschr. Phys. **13**, 385 (1965); E.P. Wigner, Phys. Rev. **77**, 711 (1950).
[29] D.D. Coon, S. Yu, and M.M. Baker, Phys. Rev. D **5**, 1429 (1972); M. Arik and D.D. Coon, J. Math. Phys. **16**, 1776 (1975).
[30] M. Arik and D.D. Coon, J. Math. Phys. **17**, 524 (1976).
[31] M. Chaichian and A. Demichev, *Introduction to Quantum Groups* (World Scientific, Singapore, 1996).
[32] R.J. McDermott and A.I. Solomon, J. Phys. A **27**, L15 (1994); A.I. Solomon, *Fifth International Conference on Squeezed States and Uncertainty Relation*, edited by D. Han, J. Janszky, Y.S. Kim, and V.I. Man'ko (NASA, Greenbelt, MD, 1998).
[33] W. Vogel and R.L. de Matos Filho, Phys. Rev. A **52**, 4214 (1995).
[34] R.L. de Matos Filho and W. Vogel, Phys. Rev. A **58**, R1661 (1998).
[35] H. Moya-Cessa and P. Tombesi, Phys. Rev. A **61**, 025401 (2000).
[36] Stephen Wolfram, *The Mathematica Book* (Cambridge University Press, Cambridge, 1999).
[37] D.M. Meekhof, C. Monroe, B.E. King, W.M. Itano, and D.J. Wineland, Phys. Rev. Lett. **76**, 1796 (1996).
[38] G.C. Hegerfeldt and T.S. Wilser, *Proceedings of the II. International Wigner Symposium, 1991* (World Scientific, Singapore, 1992), p. 104; C.W. Gardiner, A.S. Parkins, and P. Zoller, Phys. Rev. A **46**, 4363 (1992); J. Dalibard, Y. Castin, and K. Mølmer, Phys. Rev. Lett. **68**, 580 (1992).
[39] H.J. Carmichael, *An Open Systems Approach to Quantum Optics*, *Lecture Notes in Physics* (Springer, Berlin, 1993).
[40] K. Mølmer, Y. Castin, and J. Dalibard, J. Opt. Soc. Am. B **10**, 524 (1993); B.M. Garraway and P.L. Knight, Phys. Rev. A **50**, 2548 (1994); M.B. Plenio and P.L. Knight, Rev. Mod. Phys. **70**, 101 (1998).